International Research Journal of Engineering and Technology (IRJET) e-ISSN: 2395 -0056
Volume: 04 Issue: 07 | July -2017 www.irjet.net p-ISSN: 2395-0072

Using Half Pipes as Permeable Breakwater

Mohammed Ibrahim [1], Hany Ahmed [1], Mostafa Abd Alall [1]

[1]*Irrigation and Hydraulics sector, Civil Engineering, Al-Azhar University, Cairo, Egypt*

Abstract - *In terms of the importance of protecting Egyptian coastline, the hydrodynamic efficiency of the two cases of half pipes (i.e. the first case is horizontal half pipes-H shape. The second case is vertical half pipe-C shape. The draft is a decimal multiple of the total depth. The lower part is permeable with a porosity of 56, 68 and 81%) was investigated using physical models were investigated, physically and numerically by Flow-3D. The experimental work identified the hydraulic performance of the barriers. In addition, the model provided reasonable results to the contributing variables (i.e. wave height, wave length and barrier characteristics. The research concluded that increasing the relative depth (h/L) decreases the transmission coefficient (kt) and increases the reflection coefficient (kr).from FLOW-3D results able to find values velocity front and behind barriers. The numerical model is validated against laboratory data. A good agreement was apparent, where the results indicated the applicability of the numerical model to reproduce most of the important features of the interaction.*

Key Words: coastal structures - Permeable breakwater – perforated half pipes - numerical model - refraction - transmission - energy dissipation.

1. INTRODUCTION

Traditional breakwaters (i.e. rubble-mound, vertical caissons and gravity wall) are widely used to provide a protected calm water area to accommodate vessels and to allow loading and unloading processes. Such types possess a large width according to the water depth. Consequently, great amounts of construction material are required. Moreover; such breakwaters block the littoral drift leading to the occurrence of severe erosion or accretion. In addition, they dampen the water circulation leading to a deteriorated the water quality and achieving an unbalance to the ecosystem. Furthermore; traditional structures need skilled labor for their construction and certain foundation requirements. All the above leads to an uneconomic construction cost.

On the contrary, permeable breakwaters avoid the occurrence of the above side-effects, at the same time they provide reasonable protection with economic construction cost. Many researchers proposed innovative breakwaters, tested them and introduced them to practice. These types were found to have some discrepancies if were applied in Egypt. This research was thus initiated with the objective of proposing and investigating the hydrodynamic performance of an innovative economic breakwater and applicable to Egypt, experimentally and numerically. This was achieved by undergoing some research phases. These were reviewing the literature, proposing an innovative breakwater, investigating the proposed breakwater experimentally and numerically, analyzing so as discussing the results.

2. LITERATURE REVIEW

In terms of the importance of safeguarding the coastal zone in Egypt, a literature review was undertaken to perceive a clear overview to the researchers that are involved in such a topic. Therefore; many published reports, periodicals and articles in scientific journals were assembled, reviewed, analyzed and comprehended. Based on the revised literature, it was found that many researchers were involved in investigating. Abdul Khader et al. (1981) studied the hydraulic aspects of closely spaced circular cylinders as a breakwater. Dalrymple et al. (1991) investigated the reflection and transmission coefficients on a porous breakwater for normal and oblique wave incidence. The problem was solved by Eigen-function expansions theory. Kriebel (1992) investigated wave transmission and wave forces for vertical wave barriers. This type might be called wave screen or slit-type breakwater. Yu (1994) studied wave-induced oscillation in a semicircular harbor with porous breakwaters based on the linear potential wave theory and a newly derived boundary condition for the breakwaters. Isaacson et al. (1998) outlined a numerical calculation of wave interactions with a thin vertical slotted barrier extending from the water surface to some distance above the seabed. Hall et al. (2000) studied the wave transmission through multi-layered wave screens. The model was a wave screen with a porous vertical wall, Suh et al. (2007) studied wave reflection and transmission by curtain wall-pile breakwaters using circular piles. Rageh et al. (2009) investigated the hydrodynamic efficiency of vertical walls with horizontal slots. A. Schlenkhoff M. Oertel and H.Ahmed (2012) studied permeable breakwaters have been suggested to overcome the disadvantages of fully protection breakwaters. Fernández et al (2013) investigated experimentally the effectiveness of a ship used as a detached floating breakwater for coastal protection. Ahmed (2014) investigated regular wave interaction using a numerical model of (FLOW-3D, VOF) with a single vertical perforated wall.

3. INVESTIGATING THE PROPOSED BREAKWATER NUMERICALLY

This section presents the implemented model and its theory. It presents the validation process of the model

together with the executed numerical simulations to the proposed breakwater

3.1 Implemented Model

The proposed breakwater was due to be investigated. This was achieved via achieving numerical simulations using the commercial "Computational Fluid Dynamics" (CFD) code FLOW-3D. This is attributed to the fact that from the assembled literature, it was clear that CFD applications are common practice in all sectors of engineering and they are increasingly becoming important in maritime and coastal engineering. Therefore, the commercial CFD code (i.e. FLOW-3D, Flow Science Inc.) was chosen to be implemented in this study.

3.2 Theory of Flow-3d

Basically, FLOW-3D applies the finite volume theory to solve the three-dimensional Reynolds- Averaged Navier-Stokes (RANS) equations. The model is formed of a group of solid subcomponents; the numerical model within FLOW-3D represented the geometrical and hydraulic boundary conditions as shown in figure (1).

3.3 Numerical Simulations Using Flow-3D

Confident with the validation process, the model was implemented, varying the different parameters. Numerical replications were achieved to simulate the proposed breakwater. In order to get a good compromising between precision/accuracy and computation time, two independent meshes with different cell sizes were used. Mesh cells are sized by 1 cm in each direction for waves of small frequencies and mesh cells are sized by 0.5cm for waves of large frequencies. The time window for analyzing the wave height is carefully selected according to the wave length and is adjusted to avoid any reflection from the flume end or the wave paddle. The reflection coefficient was calculated by the three-probe method of Mansard and Funk (1980). The selected data are converted into frequency domain by Fast Fourier Transformation. Finally, the spectrum of the incident, transmitted and reflected wave height were calculated. Thereby, the reflection coefficient 'kr' is calculated from extracted wave profiles by:

$$kr = \frac{Hr}{Hi} \quad (1)$$

Where: Hr is the reflected wave height, Hi is incident wave height.

The transmission coefficient 'kt' was calculated directly from the wave transmitted profile by:

$$kt = \frac{Ht}{Hi} \quad (2)$$

Where: Ht is the transmitted wave height.

The energy dissipation coefficient 'kd' is given

$$k_d = \sqrt{1 - k_r^{\,2} - k_t^{\,2}} \quad (3)$$

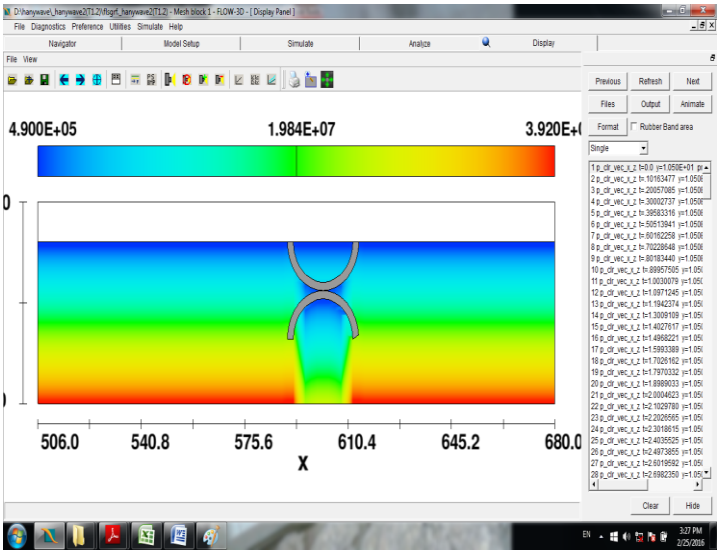

Fig -1: Breakwater model in Flow-3D

4. EXPERIMENTAL WORK

After executing numerical simulations, an experimental work was due to be carried out. This was achieved in the Irrigation and Drainage Engineering laboratory of the Faculty of Engineering, Zagazig University. The experimental work investigated the effect of breakwater shape and wave characteristics on breakwater efficiency. The results were implemented in verifying and the calibrating the numerical model results.

Two shapes of breakwaters (i.e. models) were tested in the Faculty of Engineering laboratories, Zagazig University to investigate their hydrodynamic performance. The first shape is perforated half pipe call (C shape) as figure (2-a), where the second shape is perforated half pipe call (C shape) as figure (2-b) (i.e. half pipes supported on piles); figure (2).

Driven by the importance of coastal regions that play an important role in the national income, this experimental work was achieved. This chapter presents this investigation phase under the following headlines:

(Wave flume, Wave generator, Measuring devices, Data acquisition, Tested models, Test procedures and Dimensional analysis)

(a) (b)

Fig -2: perforated half pipe supported on piles. a (C shape) and b (H shape)

4.1 wave flume

The implemented wave flume has a rectangular cross section (i.e. 2 m bed width and 1.2 m depth). The overall length of the flume is 12 m. All sides of the flume are reinforced concrete (i.e. 0.25 m thick). The flume is divided into three parts (i.e. the inlet, working section and the outlet). A 3:1 gravel wave absorber is installed at the outlet of the flume in order to absorb the transmitted waves. A general view of the flume is presented; Figure (3). Figure (4) present the details and dimensions of the models in the flume.

4.2 wave generator

The wave generator is a flap type generator. It is installed at the upstream end of flume. It consists of a hinged steel gate supported at the flume bed and connected to two steel flywheels with 0.36 m diameter by two steel rods (i.e. 1.5cm diameter and1.50m long). The system is connected to a variable speed 5 HP motor of 1400 rpm. A gearbox was used to reduce the number of revolution to range between 15 and 90 rpm in order to produce a wave period ranging between 0.60 and 4 sec.

Electronic digital inventor was used to control the generator velocity. General view and the calibration of the wave generator are presented on photo (6) and figure (7).

4.3 measuring devices

Among the measuring device is a wave gauge. It is a wave probe of standard conductivity. It is used to measure the wave elevations. The wave probe encompasses two thin parallel stainless steel electrodes. The probe consists of two 0.15 cm diameter stainless steel wires spaced at 1.25 cm and are 0.30 m long. The probe is connected to a wave monitor module in the electronic console by a twin core flexible cable. This monitor provides output signals in the form of voltage data. Static calibration of the wave probe is carried out every day at the beginning and end of each set of experiments. The calibration constants are found to have a standard deviation of less than 1.0%. An electronic converter is used for converting the analogue signals to digital voltage data. These data are collected by the personal computer and converted to the wave elevation by a simple computer program. where the water surface variation could be drawn. A general view of the standard conductivity type wave probe instrument is presented in Figure (5).

A static calibration to the wave probe is carried daily at the beginning and end of each set of experiments. The calibration constants were found to have a standard deviation of less than 1.0%.

Fig -3: General view of the wave flume

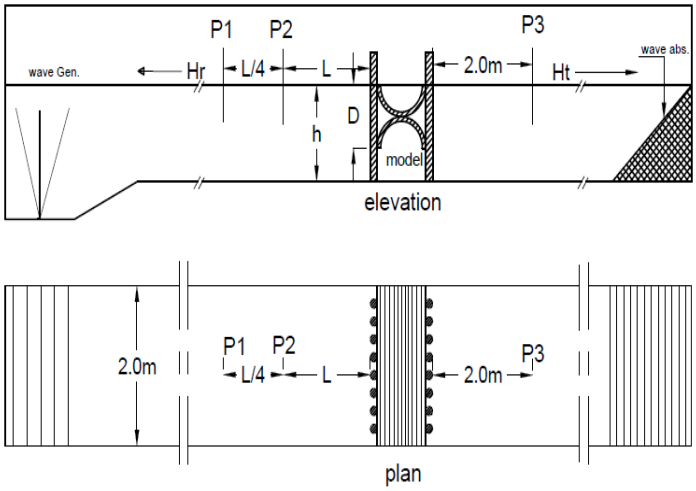

Fig -4: Definition sketch for the half pipe breakwater

Fig -5: General View of the Wave Generator

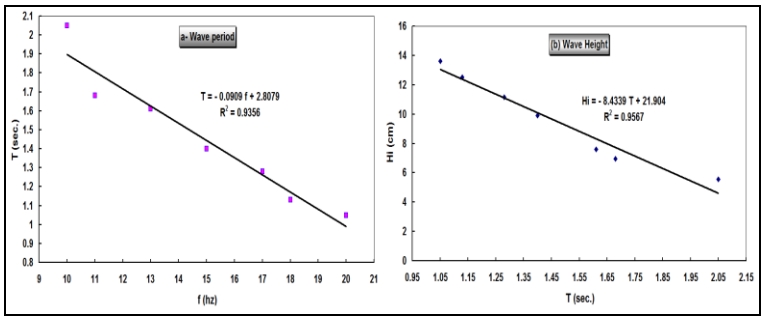

Fig -6: Calibration of Wave Generator

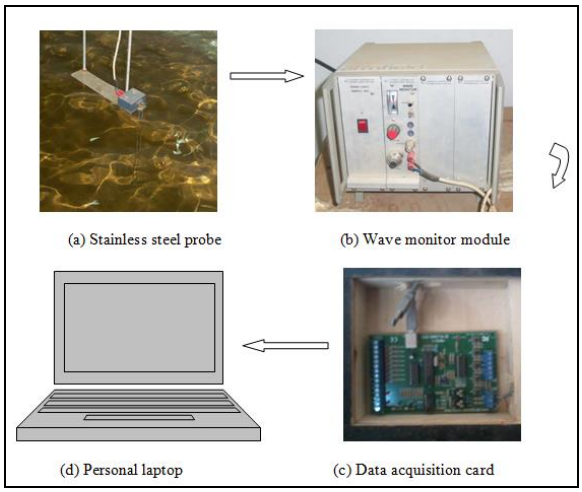

Fig -7: a general view of the Standard conductivity type wave probe

4.4 data acquisition

Each test is done three times as one probe is used. Two runs are used for separating the incident and reflected waves and the third run is used for measuring the transmitted waves. A 12 bit A/D converter was used for converting analogue signals to digital voltage data. These data are collected by the personal computer and converted to wave elevation by a simple computer program. For all the runs water surface variation was drawn against time.

4.5 tested models

Breakwater models were tested using 0.4 m water depth with different wave heights. Figure (8), figure (9) shows the isometric view of the breakwater models and their dimensions, respectively. Table (1) lists the dimensions of the tested breakwater models and the set up parameters for the models.

Fig -8: Isometric view of the tested breakwater models

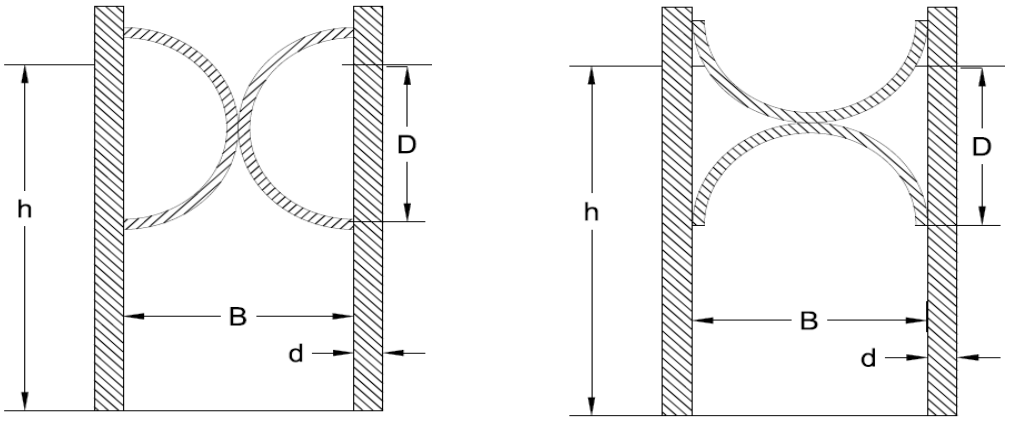

(a) C- shape (b) H- shape

Fig -9: the dimensions of the tested breakwater models. (a) C- shape and (b) H- shape

Table -1: The experimental setup parameters for the half pipe supported on piles

Parameter	The ranges	Notes
Water Depth (h) (m)	0.40	at the breakwater sit
Wave Periods (T) (sec.)	0.9 to 2	
Wave Length (L) (m)	1.21 to 3.77	at the breakwater sit
Breakwater Width (B) (m)	0.20 and 0.40	
Breakwater Draft (D) (m)	0.2 and 0.10	
Porosity (ε)	0.81 ,0.68and 0.56	Dimensionless
Wave incident (Hi)(cm)	4.2 to 12.5	
Relative depth (h/L)	0.11 to 0.33	Dimensionless
Pile diameter(d)(m)	0.06	

4.6 test procedures

The experimental models were tested using different wave periods that ranged between 0.90 and 2.00 sec, on a horizontal bed. The water height ranged between 0.15 and 0.25 m. The dimensions of the tested model are described in table (1). In order to fulfill the objectives of this research, three hundred runs (300) were executed, one hundred (100) of them were carried without models to determine incident wave height, while the rest were carried with 2 different models to record wave height upstream and downstream, by following the steps

1. Model number 1 was fixed in the middle of the flume.
2. The water depth was adjusted to be 0.4 m (h= 0.4 m).
3. The wave generator was adjusted to produce a wave period "T" of 2.00 sec (generator frequency equals 10)
4. The wave generator was operated until waves became steady and wave heights were recorded seaward so as shoreward of the model, at the selected locations; figure (2).
5. The incident (H_i) and reflected (H_r) wave heights were measured at two recording positions P_3 and P_2 ($\eta_{max.}$ at location P_3).
6. The quasi-antinode $\eta_{min.}$ at location P_2 and the quasi-nodes are set in front of the breakwater model (wave generator side). The positions P_3 and P_3 are located at distances L and 1.25 L, respectively (i.e. L is the wavelength that varies according to the wave period T), ***Dean and Dalrymple (1984)***.
7. The extreme values of water elevation η(x) for any location x, was estimated using the following relation:

$$\eta(x) = \pm\sqrt{(H_i/2)^2 + (H_r/2)^2 + (H_i H_r/2)\cos(2kx+\varepsilon)} \quad (1)$$

Where:

k = the wave number (k=2π/L)

ε = the phase lag induced by the reflection process

η(x) varies periodically with x and it becomes a maximum of the envelope at the phase positions (2kx1+ε)=2nπ, n=0, 1, 2, …

η(x) max. = (Hi + Hr) / 2 the quasi-antinodes (2)

Whereas at the phase positions, (2kx2+ε)=(2n+1)π, n=0, 1, 2, …, it becomes a minimum of the envelope, as follows:

η(x) min. = (Hi - Hr) / 2 the quasi-antinodes (3)

8. The distance between the quasi-antinodes and the quasi-nodes was determined by subtracting the phases as x2 – x1 = L / 4.
9. The incident (Hi) and reflected (Hr) wave heights were estimated using the following relation:

Hi = ηmax. + ηmin. (4)

Hr = ηmax. - ηmin. (5)

10. The transmitted wave heights (Ht) were measured by recording one additional measure, at position (P1), behind the breakwater model (i.e. at wave absorber side) at a distance 2.0 m form the shore side of the breakwater. This was achieved in order to avoid the effect of the turbulence caused by the wave overtopping on the breakwater and to minimize the effect of the wave reflection from the wave absorber at the end of the flume. Figure (2) presents the details of the wave flume, position of the tested breakwater models and wave recording locations.
11. The reflection (kr) and the transmission (kt) coefficients were estimated using the following relations:

kr = Hr / Hi (6)

kt = Ht / Hi (7)

12. The energy equilibrium of an incident wave attacking the structure was determined using the following relation:

Ei = Er + Et + Ed (8)

Where:

Ei = the energy of incident wave ($E_i=\rho g H_i^2/8$)

ρ = the water density

g = the acceleration due to gravity

E_r = the energy of reflected wave ($E_r=\rho g H_r^2/8$)

E_t = the energy of transmitted wave ($E_t=\rho g H_t^2/8$)

E_d = the wave energy dissipation.

13. The dissipation coefficient was determined by substituting in equation (8) by values of E_i, E_r, E_t and dividing the result by E_i, which yields:

$$1 = \left(\frac{H_r}{H_i}\right)^2 + \left(\frac{H_t}{H_i}\right)^2 + \frac{E_d}{E_i} \quad (9)$$

And substituting in equations (6) and (7) in equation (9). The wave energy dissipation coefficient $k_d=(E_d/E_i)^{1/2}$ was estimated as follows:

$$k_d = \sqrt{1 - k_r^2 - k_t^2} \quad (10)$$

14. The previous steps were repeated for the other models of the new dimensions and wave periods of T=2, 1.9, 1.7, 1.5, 1.40, 1.3, 1.1 and 0.9 sec, where the wave heights were recorded.

5. RESALTS OFHALF PIPE WAVE INTERACTION

The hydrodynamic efficiency of the two cases of half pipes (i.e. the first case is horizontal half pipes-H shape. The second case is vertical half pipe-C shape. The draft is a decimal multiple of the total depth. The lower part is permeable with a porosity of 56, 68 and 81%) was investigated using physical models.

The breakwater efficiency is presented as a function of transmission, reflection, and wave energy dissipation coefficients. The effect of different wave and structural parameters (i.e. the wave length, the half pipe draft, width and porosity) on the breakwater efficiency is investigated. Its hydrodynamic efficiency is experimentally studied.

The hydrodynamic efficiency of the breakwater is evaluated by calculating the wave transmission, reflection and energy dissipation coefficients for different wave and structural parameters. The results indicated that the transmission coefficient is inversely proportional to relative wave lengths (h/L and B/L), wave steepness (Hi/L) and relative breakwater width (B/h). It is directly proportional to the relative draft (D/h). While the reflection coefficient and the dissipation coefficients follow an opposite trend. The efficiency of the second case is better than the first by about 5 to 25%. In addition, increasing the porosity improves the breakwater efficiency.

In addition, numerical model (FLOW-3D) was implemented for estimating the transmission and reflection coefficients. The results were compared to the experimental and theoretical results of other researchers, where it indicated a reasonable agreement. In addition, the breakwater provided a better efficiency when compared to other breakwater configurations.

5.1 numerical model verification

The numerical model is validated against laboratory data. A good agreement was apparent, where the results indicated the applicability of the numerical model to reproduce most of the important features of the interaction, charts (1) and (2).

5.2 half pipe breakwater porosity and shape

Chart (3) presents a comparison between (H-shape) and (C-shape) experimental results for the different dimensionless parameters (h/L) at porosity =81%, D/h=0.25 and B/h=0.5. The chart indicated that for (C-shape), kt decreased by increasing h/L from 0.78 to 0.23, where h/L increased from 0.11 to 0.33 at B/h=0.5 and D/h=0.25. For the (H- shape), the transmission coefficients (kt) decreased from 0.83 to 0.43 when h/L increased from 0.11 to 0.33, at the same parameters. While the reflection coefficients (kr) increased by decreasing h/L.

For (C-shape), (kr) increased from 0.22 to 0.68, when h/L increased from 0.11 to 0.33. For (H-shape), (kr) increased from 0.33 to 0.67, when h/L increased from 0.11 to 0.33.

The coefficient (kl) for (C-shape) increased from 0.26 to 0.48. and that of (H-shape), it increased from 0.20 to 0.36. Based on the obtained results, it was clear that (C- shape) is better than (H-shape) by 5% to 20%.

From chart (4) indicated that the (C-shape) provided a better result, at D/h=0.50 rather than D/h=0.25 by 11% to 20%.In the same context. On the other hand, chart (5) indicated that the (H-shape) provided a better results at porosity =0.56 rather than porosity=0.81 so as 0.68 by 26% to 48%.

5.3 VELOCITY DISTRIBUTION

The numerical model was implemented to detect the velocity field and the velocity vectors in the vicinity of the barriers. This was achieved to indicate how energy was dissipated.

Chart (6) presents the velocity vector and velocity field, provided by FLOW-3D, for time increment of 0.1 sec of wave period 1.10 sec. The higher velocities were observed at the wave crests around the slots. The higher velocities are formed through the slots due to the presence of the obstacle, which causes contraction of moving wave. The velocity magnitude is very high in front of the barrier and very low behind it, where a part of wave energy is banned, another part is transmitted and the rest part is dissipated, as a vortex as presented by the velocity vectors. The transmitted part is redistributed along the total depth beyond a distance equals the water depth. The surrounding area of the barrier is considered by Flow-3D, while other areas are considered to be 2-dimensional flow. The flow within the area between the barriers is turbulent and the motion seems to be vertical, except for the region located near the slots.

A half perforated pipes for (H-shape) and (C-shape) at B/h, D/h=0.50. The mean velocity field in the breakwater area is presented on chart (7), where (a)-t=20.25T, (b)-t=20.50T and (c)-t=20.75T over the 20th wave cycle. The maximum velocity for (H-shape) is 100 cm/s. This was observed in the region of the half pipe; chart (7). This occurred mainly in the seaward side of the structures, where the main structure-interaction takes place and intense vortices are observed. A recirculating region is observed in the region beneath the body of each barrier with the first one being stronger and wider the mean velocity field for permeable barriers with porosity 0.50

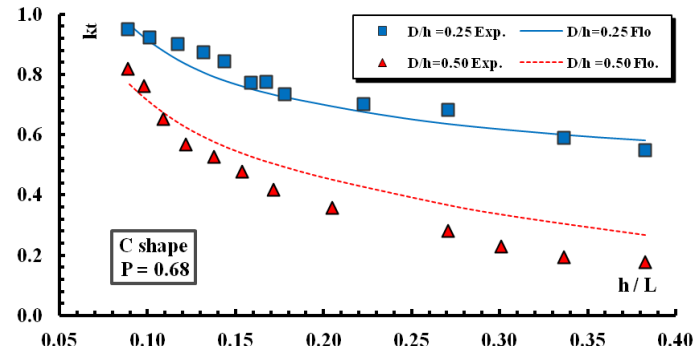

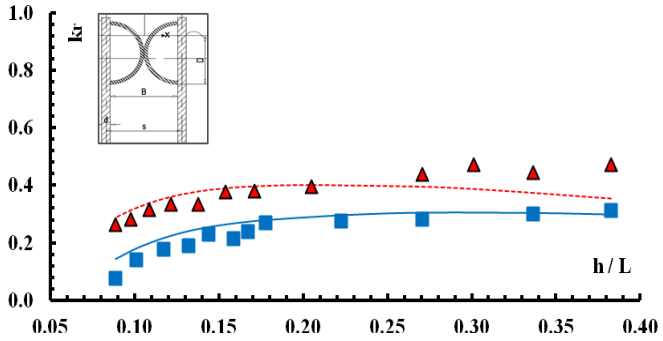

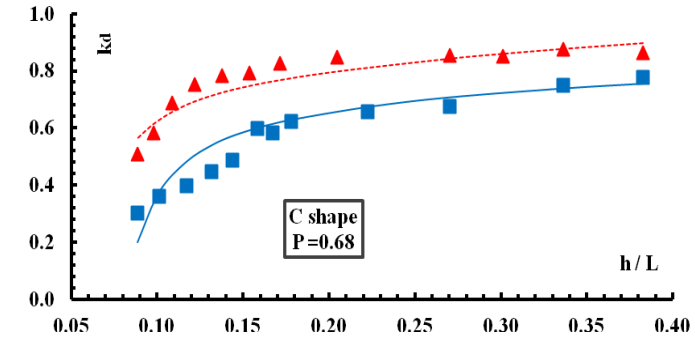

Chart -1: Comparison between Experimental and Flow-3D results for different values of (D/h) at porosity = 68 % (C-shape)

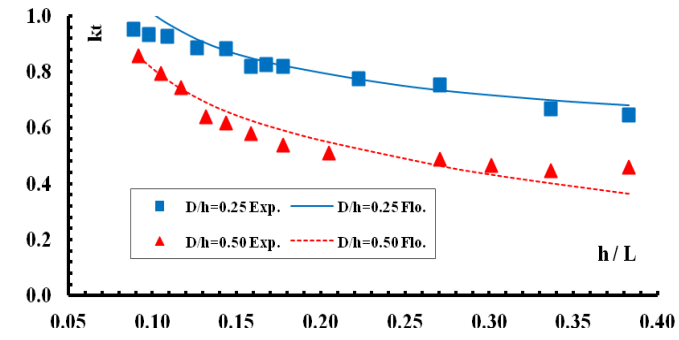

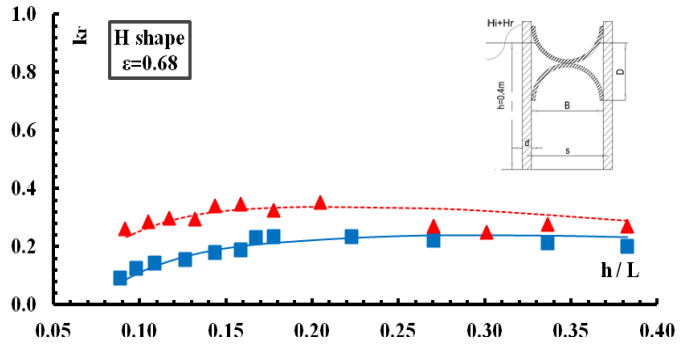

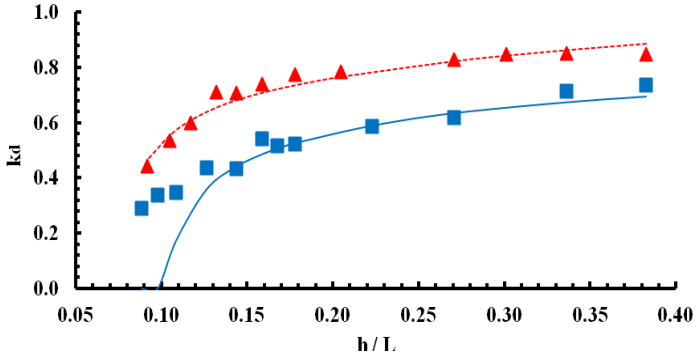

Chart -2: Comparison between experimental and Flow-3D results for different values of (D/h) at porosity = 68 % (H-shape)

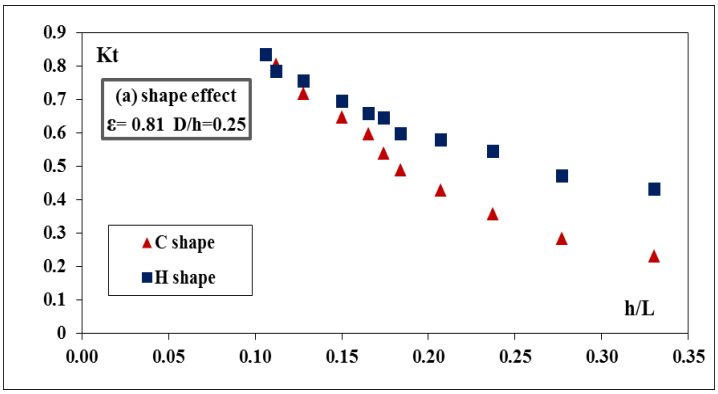

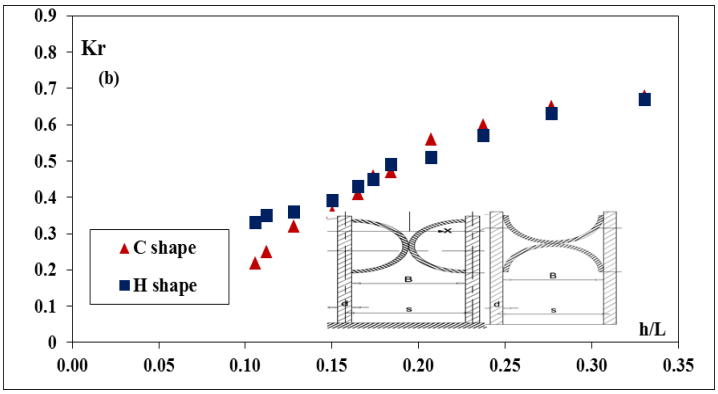

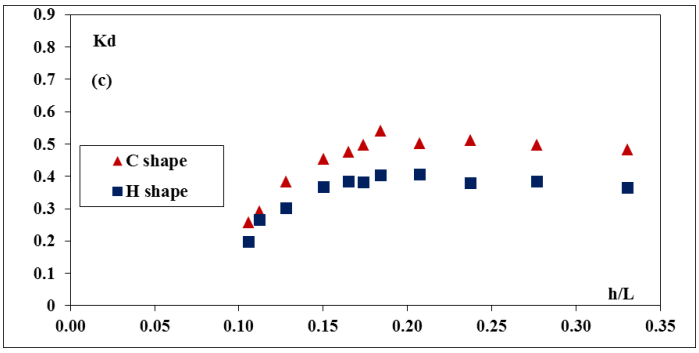

Chart -3: Comparison between (H-shape) and (C-shape) experimental results for (h/L) at porosity (ε) =81%, D/h=0.25 and B/h=0.5 (a)kt, (b)kr and (c) kd

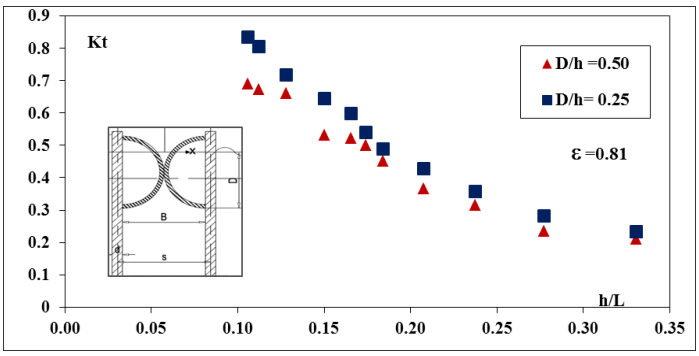

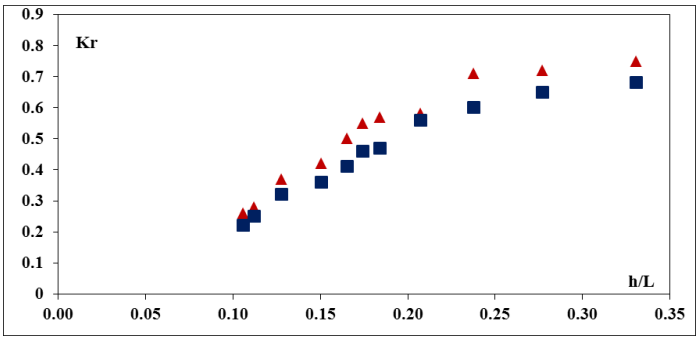

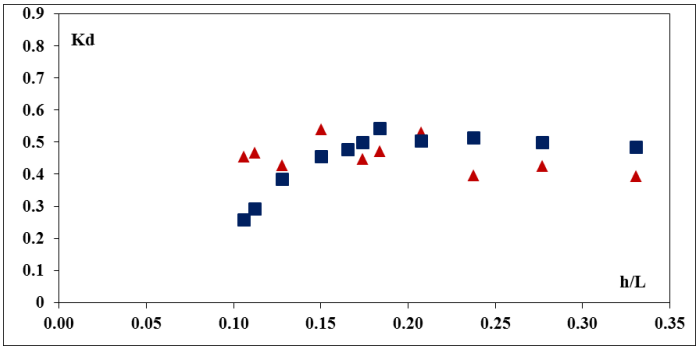

Chart -4: Effect of (C-shape) on Kt, Kr and Kd for different (D/h) at (ε)=81% and B/h=0.5

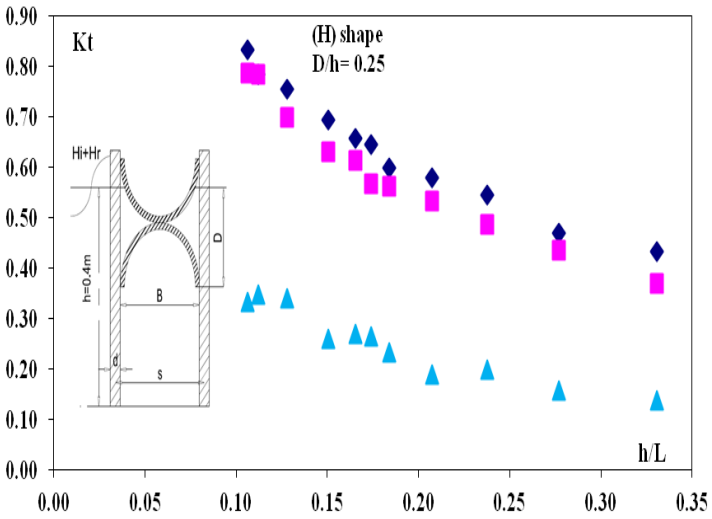

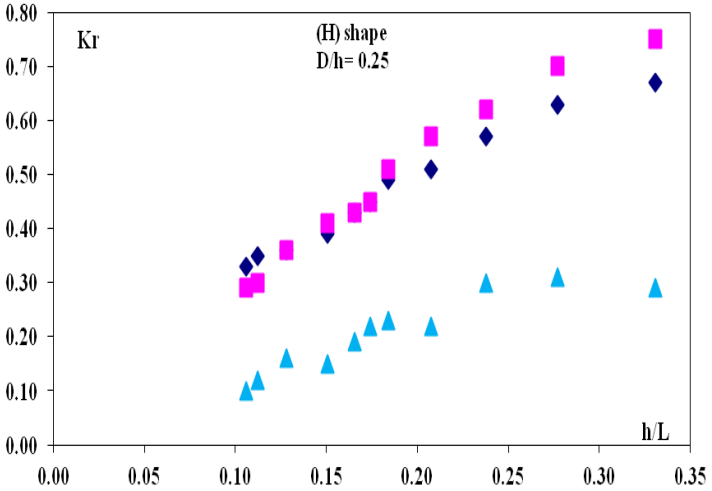

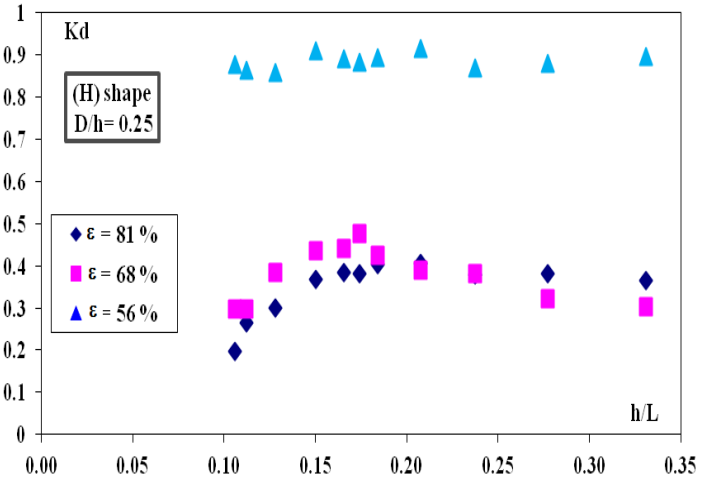

Chart -5: Effect of (H-shape) on Kt, Kr and Kd for different values of (ε) at D/h=0.25, B/h=0.5

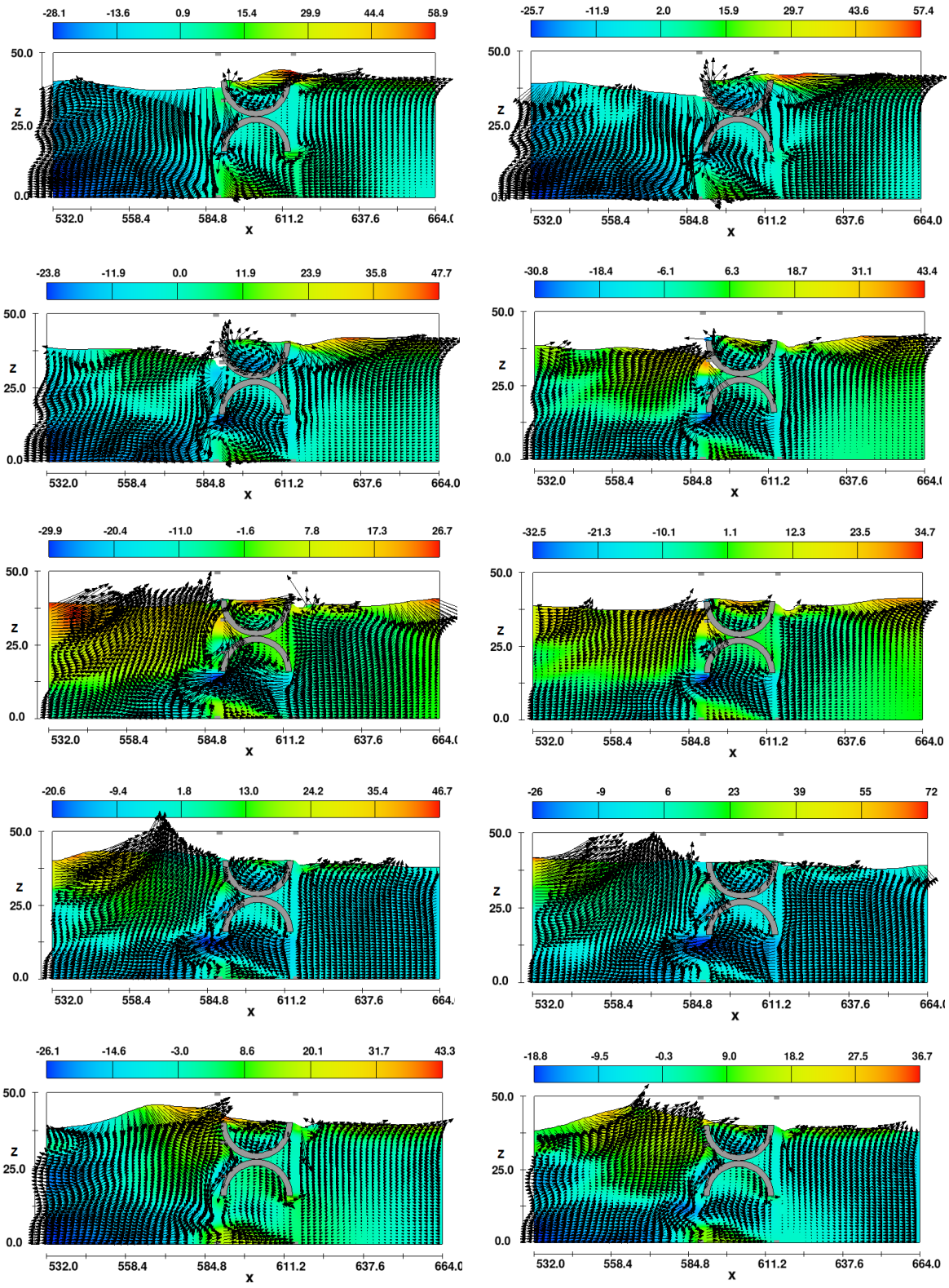

Chart -6: Velocity magnitude (cm/s) and velocity vector by FLOW-3D for half pipe (H-shape) at = (12:13)sec for T= 1.1 sec, *hi* = 10 cm, *dt* = 0.1 sec B/h=0.50

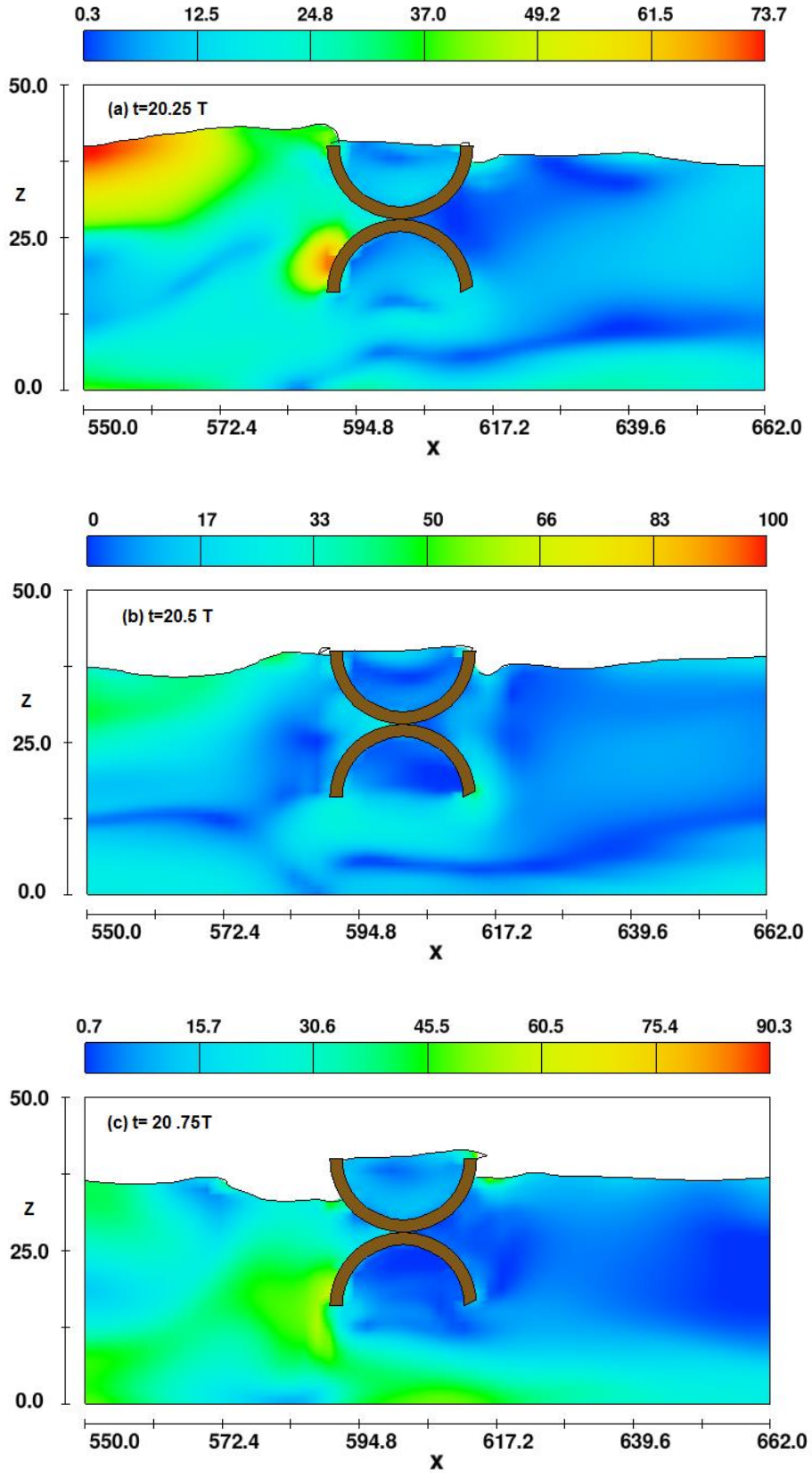

Chart -7: Detailed velocity field in the region of the Half pipes (H-shape) Porosity=0.50,B/h=0.5 and Hi=9 cm-T=1.20 sec

6. CONCLUSIONS

The following are the deduced conclusions from the present research:

For the 2 permeable half pipes (H-shape) and (C-shape) breakwaters, the following were detected:

The proposed innovative breakwaters could be simulated numerically, via FLOW-3D, as the experimental and numerical results indicated confident agreement.
The (C-shape) proved to dissipate more energy than the (H-shape) breakwater by 5-20%.
The permeability of piles at 56% reduces the transmission of waves by 68-81%.
The increase of draught increases the reflection coefficient.
The comparison between the present experimental results and previous researches results indicated favorable agreement

For the velocity distribution fields near the investigated innovative breakwaters, the following were observed:

Higher velocities are observed at the crest of wave and around the slots.
Higher velocities are formed through slots due to the effect of obstacles.
The velocity magnitude is very high in front of the barrier and very low behind it.
The flow between the barriers is turbulent and the motion is vertical, except for the region near the slots.

REFERENCES

[1] Abdul Khader, M. H. and Rai, S.P., 1981. "Wave attenuation due to closely spaced circular cylinders.", Proc. of the International Association for hydraulic Research, XIX Congress, New Delhi, pp. 93-102.
[2] Kriebel, D. L., 1992. "Vertical wave barriers: Wave transmission and wave forces." 23rd Int. Conf. on Coastal Eng., ASCE, Vol.2. pp. 1313-1326
[3] Yu1994. "Wave induced oscillation in harbour with porous breakwaters", J. of Waterway, Port, Coastal and Ocean Eng., Vol. 120, No. 2, pp. 125-144.
[4] Isaacson, M., Premasiro, S. and Yang, G., 1998. "Wave interaction with vertical slotted barrier." Journal Waterway, Port, Coastal and Ocean Eng., Vol. 124, No. 3, pp. 118-126.
[5] Hall, K., 2000. "Wave Transmission Through Multi-layear Wave Screens." MS.c. thesis at Queen's University, Kingston, Ontario, Canada.
[6] Rageh, O. S. and Koraim, A. S., 2009. "The use of vertical walls with horizontal slots breakwaters." 30th international water technology conf., IWTC 13, Hurghada, Egypt.
[7] Suh, K. D., Jung, H. Y. and Pyun C. K., 2007. "Wave reflection and transmission by Curtain wall-Pile breakwaters using circular piles." J. of waterways, Port, Coastal and Ocean Eng., Vol.34, Issues 14-15, pp. 2100-2106.
[8] Rageh, O. S. and Koraim, A. S., 2009. "The use of vertical walls with horizontal slots breakwaters." 30th international water technology conf., IWTC 13, Hurghada, Egypt.
[9] Fernández L. A., Gutiérrez S. , V. Negro and J.S. López (2013) "Use of a scrapped ship as a floating breakwater for shore protection" J. Coastal Research, Special Issue No. 65.
[10] Ahmed, 2014 "Stokes second-order wave interaction with vertical slotted wall breakwater." Coastal structures conference. Yokohama, Japan, 2011.